

Photoelectrochemical Studies on Inorganic/Organic Aqueous Nano-Suspensions Made by TiO₂/Poly Neutral Red Assembly

Kasem K. Kasem* and William Bennett

School of Science, Indiana University Kokomo, Kokomo, IN, 46904, USA

Abstract: An inorganic/organic interface (IOI) consisting of TiO₂/polyNeutral Red(PNR) was subjected to photoelectrochemical studies in both aqueous nano-suspensions and in thin solid forms. The effects caused by PNR modifier on the photoelectrochemical behaviour of the IOI were investigated using [Fe(CN)₆]⁴⁻ as a photoactive hydrated electron donor agent. Results show that the adsorption process of [Fe(CN)₆]³⁻ (photolysis product) controls the photo-activity outcomes of IOI assemblies. TiO₂/PNR shows lower heterogeneous photochemical response than native TiO₂ in a short photolysis time. At longer photolysis times the IOI show a photo activity greater than that of native TiO₂. TiO₂/PNR nanoparticles adsorb more [Fe(CN)₆]³⁻ in a very steady adsorption /desorption process than the unmodified particles. The interface activities were explained by analysing the IOI junction characteristics, such as electron affinity, work function and hole/electron barrier heights. At TiO₂/PNR a strong hybridization between electrons-like and hole-like sub band states in close vicinity to the Fermi energy are developed. The aqueous nano-systems retained moderate stability as indicated by the reproducibility of their photo catalytic activities. Both [Fe(CN)₆]⁴⁻ and PNR contributed to the stability of native TiO₂ surfaces.

Keywords: Poly Neutral Red, Inorganic Organic Interface, Modified TiO₂ Surface Photoelectrochemistry.

Introduction

Nanostructured assemblies consisting of inorganic–organic interfaces (IOI) were the focus of attention of several investigations in the field of solar energy¹⁻¹⁰. A special class of these IOI is dye-sensitized semiconductors. Photocatalytic hydrogen production by dye-sensitized Pt-SnO₂ and Pt-SnO₂, RuO₂ in aqueous methyl viologen solution was reported¹⁻⁴.

Photoelectrochemical studies that involved electro-chromic devices⁵ and solar cells⁶⁻⁸ were performed. Furthermore, efficient hydrogen evolution using a merocyanine dye-sensitized Pt-TiO₂ photocatalyst under visible light irradiation was previously studied⁹. The kinetics of the charge transfer at these IOI was further investigated¹⁰. A number of semiconductors in the form of thin film electrodes or colloidal systems, which might be used in solid or liquid photovoltaic cells, were investigated¹¹⁻¹⁴. Some metal chalcogenides modified with poly aniline, poly payroll, or other organic semiconductors were studied¹⁵⁻²⁰ Special assemblies of narrow band gap semiconductor nanostructures can be convenient systems to capture visible light energy. Metal / chalcogenide/oxide semiconductors absorb only solar radiation that matches their band gap.

*Corresponding author: Kasem K. Kasem

E-mail address: kkasem@iuk.edu

DOI: <http://dx.doi.org/10.13171/mjc.3.3.2014.20.05.15>

However, useful spectrum can be widened if the surfaces of the metal sulfides are modified with agent/s that can absorb or become excited by greater radiation energies such as UV. Some conjugated organic semiconductors absorb UV radiation and then re-emit radiation at longer wave lengths.

Surface modification can create or eliminate defects and alter the energy band structure of the modified surface, and consequently alter the donor /acceptor character of the IOI assemblies. Recent studies show that binary oxides can provide more efficient charge separation, increased lifetime of charge carriers and enhanced interfacial charge transfer to absorbed substrates²⁰. Studies had been conducted on the photocatalytic activity using the binary semiconductor oxide systems such as CdS/AgI, and ZnO/ZnS²¹. The effect of doping metal oxides with another metal oxide was explained in some systems by creation of oxygen vacancies in the lattice of the studied assemblies' structures²².

The structure and redox behavior of the dye 3-amino-7-dimethylamino-2-methyl phenazine, known as Neutral Red (NR), has a promising role in mediating photon/charge transfer process. The fact that NR can be electro-polymerized to generate polyNeutral Red (PNR) adds another advantage of using this dye in an immobilized phase. Both electrochemical data and spectroscopic data indicate that the band-energy map of PNR can generate either straddling or staggered band alignment with some known metal oxide semiconductors in IOI assemblies. Such band alignments can facilitate and/ or coordinate the photo activities of both organic and inorganic semiconductors leading to greater capturing of incident photons at this IOI assembly. In this paper, we investigated the electrochemical and photoelectrochemical behavior of PNR and the role of PNR as a dye sensitizer on the band alignment of an IOI assembly consisting of TiO₂ nanoparticles/PNR. The effectiveness of this IOI will be judged by its contribution to photo-reduction of [Fe(CN)₆]³⁻ which generates [Fe(CN)₆]⁴⁻ as hydrated electron source during the photolysis of aqueous suspensions employing this IOI.

Experimental Section

Reagents

All the reagents were of analytical grade. All of the solutions were prepared using deionized water, unless otherwise stated. TiO₂, TiO₂ / PNR were either in nano particulate form or thin solid films.

Preparation of TiO₂ / PNR / interface

Colloidal suspensions of TiO₂/PNR interface were prepared as follows: 0.05 g of TiO₂ nanoparticles prepared as reported previously²³ were suspended in the solution of NR in acetonitrile. The mixture was subjected to a 10 minute sonication followed by stirring for one hour to allow maximum adsorption of NR on the TiO₂ nanoparticles. The excess NR was removed by centrifugation. For photo-polymerization of NR adsorbed on TiO₂ nanoparticles, TiO₂ with adsorbed NR was re-suspended in di-water containing few drops of H₂O₂ and subjected to UV radiation under constant stirring for 3 hours. The resultant TiO₂ /PNR was rinsed with deionized water several times and allowed to dry at 120 °C for 2 hours.

Deposition of thin solid films: Electrodes with thin solid films of TiO_2 particles, modified with PNR (prepared as described in 1), were suspended in an acetonitrile solution of poly vinyl pyridine (PVP). The suspension was evenly spread over an FTO (Fluorine doped Tin Oxide, Hartford Glass, Inc, IN) slide (12.5 x75 mm) and dried at 120°C for 6 hours (Diagram 1). The assembled electrode was transferred to a three-electrode cell containing the chosen buffer as the electrolyte and an Ag/AgCl and a Pt electrode as reference and a counter electrode respectively.

Instrumentation: All electrochemical experiments were carried out using a conventional three electrode cell consisting of a Pt wire as a counter electrode, a Ag/AgCl as a reference electrode, and Pt gauze as an electron collector. A BAS 100W electrochemical analyser (Bioanalytical Co.) was used to perform the electrochemical studies. Steady state reflectance spectra were performed using Shimadzu UV-2101 PC. Irradiation was performed with a solar simulator 300 watt xenon lamp (Newport) with an IR filter.

Photolysis cell: The electrolysis cell was a one-compartment Pyrex cell with a quartz window facing the irradiation source²⁴. The working electrode, a 10.0 cm^2 platinum gauze cylinder, had a solution volume of 100 mL. Suspensions were stirred with a magnetic stirrer during the measurements. Ag/AgCl/ Cl^- reference electrode was also fitted into this compartment. A 10-cm^2 platinum counter electrode was housed in a glass cylinder sealed in one end with a fine porosity glass frit.

Photolysis of $[\text{Fe}(\text{CN})_6]^{4-}$ will generate hydrated electrons and $[\text{Fe}(\text{CN})_6]^{3-}$. The potential of the working electrode was fixed at 100 mV more negative than the reduction potential of $[\text{Fe}(\text{CN})_6]^{3-}$ to guarantee full reduction of ferricyanide. The current due to the reduction of $[\text{Fe}(\text{CN})_6]^{3-}$ collected by the working electrode during the photolysis process is a measure of photocurrent. The measured photocurrent was normalized considering two photons per one hydrogen molecule, and was used to calculate the number of moles of hydrogen generated per square meter per hour of illumination.

Results and Discussion

Electropolymerization of NR

Generation of thin solid film has been achieved by repetitive cycling of the FTO electrode potential at a scan rate 0.10V/s between -0.5 and 1.5 V vs Ag/AgCl in 0.5M KCl (pH 2) containing 1 mM of NR. The results are displayed in Figure 1. The growth of the redox wave in the potential range 0 to -0.5 V (as illustrated by the up arrow in figure 1) was indicator for the build-up of PNR films.

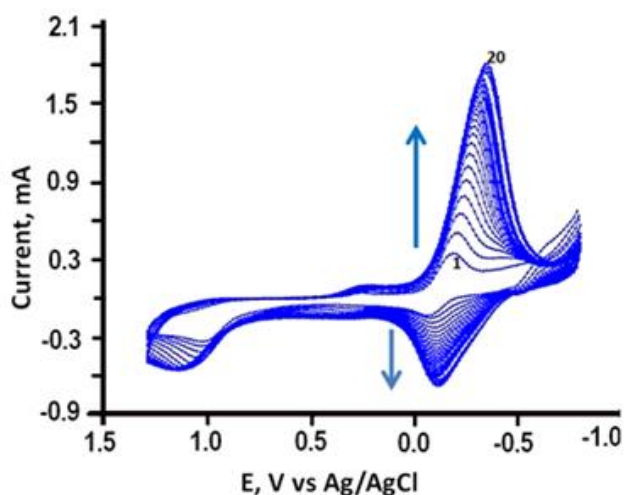


Figure 1: Electrochemical polymerization of 1 mM NR on ITO in 0.5 M KCl (pH 2) Scan rate 0.100V/s, 1 and 20 refer to scan numbers

Electrochemical behaviour of PNR

The electrochemical behavior of PNR was investigated by cycling of the FTO/ PNR electrode potential at a scan rate 0.10V/s , between -1.0 to 0.6 V vs Ag/AgCl in 0.5M KCl at pH 2 and pH 6.8. The results are displayed in Figure 2. It can be noticed that one redox system is shown in this figure with a formal potential ≈ -0.150 V vs Ag/AgCl at pH 2. This redox wave is due to the hydrogenation of N atoms in pyrazine ring of the monomer. Increasing the pH to 6.8 shifted the formal potential of the redox wave to a more negative potential (Figure 2b). Furthermore, it is worth noticing an irreversible oxidation peak at 0.8 V vs. Ag/AgCl. This highest oxidation potential is the onset oxidation potential E_{ox} of PNR as indicated in Figures 1 and 4. The value of the relative onset oxidation potential, E_{ox} , of PNR will be used to calculate the ionization potential of the PNR ²⁵.

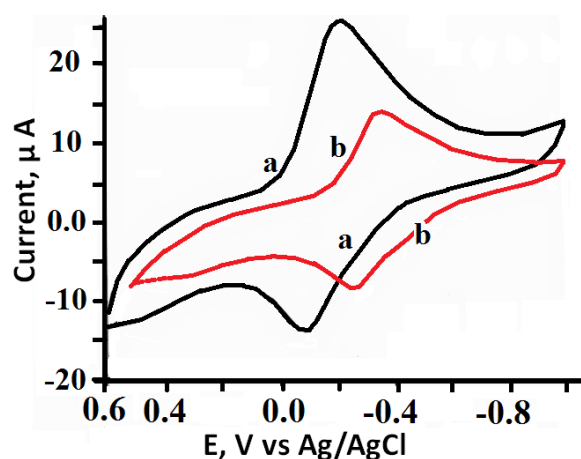


Figure 2: CV of FTO/PNR in KCl a) at pH 2, and b) at pH 6.8. Scan rate 0.100V/s.

Absorption Spectra of PNR

Absorption spectra of NR and PNR over FTO electrode were studied and the results are displayed in Figure 3A and B. Figure 3A indicates that the monomer shows absorbance peaks

at 460 and 525 nm, while the polymer spectra (Figure 3B) shows a broad or overlapped absorbance peak in the range between 430 to 550 nm. Such results are an indication of the energy intervals with high density states that represent higher occupied molecular orbitals (HOMO) and lower unoccupied molecular orbitals (LUMO) of NR ranging between 2.76 and 2.36 eV. Such absorption behaviour can be attributed to the active phenazine-ring group on the monomer²⁶. Notably, Figure 3A also shows the emission band at 590 nm after monomer excitation with 470 nm light. The emitted photons at 590 are recycled again to generate more e/h centres at the IOI assembly.

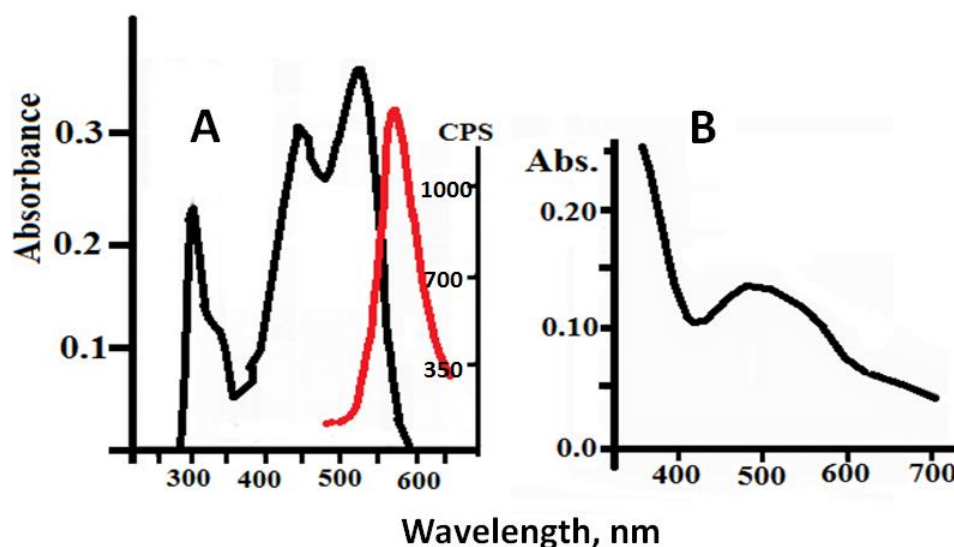


Figure 3: A) NR absorption spectra (Red curve is the fluorescence of NR, excitation with 470 nm light source B) PNR absorption spectra .

Band-energy map of PNR

Ionization potential (IP) and Electron Affinity (EA) are important parameters to draw the energy map of PNR along with the band gap (E_g). These parameters are also needed to explain the electrical and optical properties of the film. Relating electrochemical data, such as the onset oxidation potential (E'_{ox}), the onset reduction potential (E'_{Red}), and the band gap leads to an understanding of the integrated energy diagram of the film. Onset potentials can be estimated from the intersection of the two tangents drawn at the rising oxidation current and the background current in the CV using the following formula²⁵:

$$E_{SHE} \approx E_{vac} + 4.6 \text{ V} \quad 1$$

An Ag/AgCl was used as a reference electrode ($E^0 = 0.197 \text{ V} \approx 0.2 \text{ V vs SHE}$), therefore $E_{Ag/AgCl} \approx E_{SHE} + 0.20$, and when $E_{vac} \approx 0$, the above equation can be rewritten as follows:

$$E_{Ag/AgCl} \approx E_{SHE} + 0.20 \approx E_{vac} + 4.8 \text{ V} \quad 2$$

As $IP = E_{ox}$ where E_{ox} is oxidation potential onset.

$$\text{When} \quad E_{ox} = IP = E'_{ox} + E_{Ag/AgCl} \quad 3$$

Where E'_{ox} is oxidation potential onset relative to Ag/AgCl. Substitution from equation 2 to 3, results in :

$$IP \approx eE'_{ox} + E_{vac} + 4.8 \text{ eV} \quad \text{or}$$

$$IP = eE'_{ox} + 4.8 \text{ eV} \quad 4$$

Considering the energy gap between HOMO (valence band) and LUMO (conduction band) to be the band gap (E_g), and the energy gap between the LUMO and vacuum level to be the electron affinity (EA), we can write the following equation:

$$IP = EA + E_g \quad 5$$

By integrating the data obtained from Figures 1-4 and equations 1-5, a list of photo-electrochemical data for TiO_2 and PNR were deduced as well as summarized in Table 1. The quantities listed without sign to reflect only the magnitude. The fact that the hole barrier height is large ($\approx 2 \text{ eV}$) and greater than the electron barrier height may indicate that charge injection is mediated at the IOI interface through hole transfer.

Table 1: Photo-electrochemical data at TiO_2 / PNR Interface

Property , eV	TiO_2	PNR
Onset Oxidation potential (vs, Ag/AgCl)		0.8 V, vs Ag/AgCl
Measured band gap, Ea	3.0	≈ 2.48 (average)
Ionization potential IP,		5.6
E_{fb} , vs NHE	-0.20	0.05
Work function Φ	7.30	
Electron Affinity EA	4.30	2.92 (pH 6.8)
Holes' attraction forces (Barrier height) , ϕ_h at IOI *		2.0 (pH 6.8)
Electrons 'Barrier Height, ϕ_e at IOI		1.22
Life –time of excited state, ns		1.12
$\Delta EA = EA_{TiO_2} - EA_{PNR}$, eV	1.38	

- Calculated from $\phi_h = \text{Organic IP} - \Phi$ (metal oxide)

Photoelectrochemical Studies on PNR Thin Films

Cycling of the FTO electrode potential between -1.0 to 0.6 V vs Ag/AgCl in 0.5M KCl at pH 2 took place in dark and under illumination. The results are displayed in Figure 4. It can be noticed that under illumination, at potential more negative to $\approx -0.150 \text{ V}$ vs Ag/AgCl (or 0.05 V vs NHE) a larger photocurrent is reported as shown in the inset of Figure 4. This indicates that the donor states energy level (E_{fb}) is positioned within this potential range.

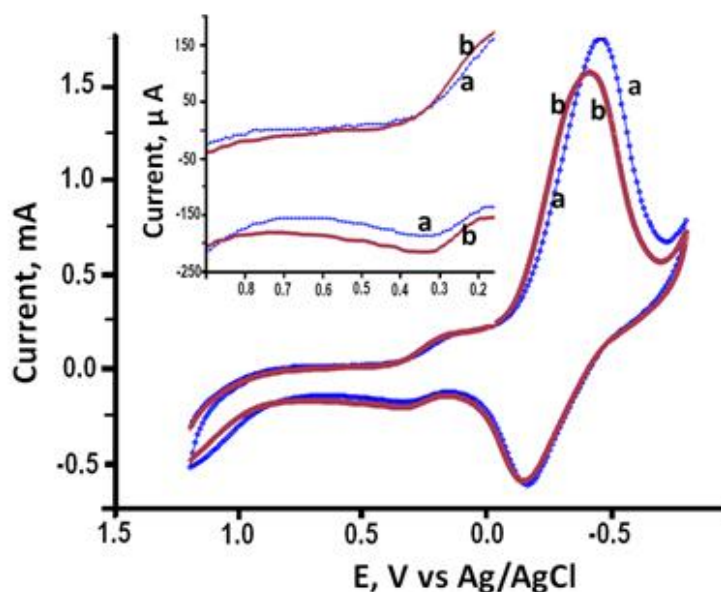


Figure 4: CV of ITO/ PNR at 0.05 V/s in 0.50M KCl (pH 2) a) dark , b) Under illumination Inset (exploded view illustrates the approximate value of E_{fb})

The low EA for PNR indicates (electron donor) p-type nature of this polymer. Furthermore, based on the calculated 2.48 eV for PNR band gap, the approximate positions of its LUMO and HOMO are at -1.68 V and 0.8 V vs Ag/AgCl respectively. The reduction of the protonated polymer takes place in two steps; protonation step followed by electron transfer step. This creates the range of energy levels in the LUMO and explains the approximation of LUMO position in the electrochemical scale. This also explains the lack of a defined reduction wave in the CV of the PNR. On the other hand, the measured E_{fb} for TiO₂/PNR was found to be 0.442 V vs NHE. Combined with the previously reported data²⁷ showing that E_{fb} for TiO₂ at pH =6 is -0.2 V vs NHE, we can conclude that the energy band alignments for TiO₂ and PNR in TiO₂/PNR assembly is of staggered gap type (Figure 5B) where a strong hybridization between electron-like and hole-like sub band states near the Fermi energy was developed. The fact that HOMO is in more negative potential (2.1 eV) than that of the TiO₂ conduction band, suggests that the charge injection is facilitated by hole transfer from TiO₂ VB to PNR HOMO to oxidize adsorbed phosphate ions. Exciting the IOI assembly with $\lambda \geq 400$ nm will cause reformation in the LUMO bands of PNR (Figure 5A). Electron injection from these reformed LUMO can causes reduction process to take place.

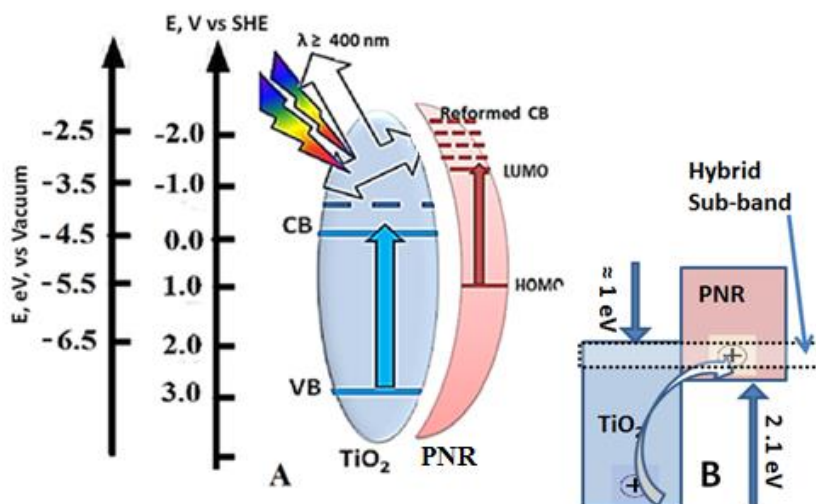


Figure 5: Energy map and band alignments of TiO₂/PNR assembly;
 A) Energy level B) Energy band alignment between TiO₂/PNR

Photoelectrochemical Behaviour of TiO₂/PNR Aqueous Suspensions

The theory of the photolysis of aqueous [Fe(CN)₆]⁴⁻ has been discussed elsewhere²⁸. In this study, aqueous suspensions of pure TiO₂ and TiO₂ surface-modified with PNR in 0.2 M phosphate buffer at pH 6 containing 0.02M [Fe(CN)₆]⁴⁻ were subject to the photolysis process. The potential of the Pt collector electrode was kept constant at 0.000 V vs Ag/AgCl. The results are displayed in Figures 6 and 7. The recorded photocurrent in this figure is due to the electrochemical reduction of K₃ [Fe(CN)₆]. In the presence of illuminated native or surface-modified TiO₂/PNR, the reduction of [Fe(CN)₆]³⁻ can take place by an electrochemical and/or by a photochemical process. However, the collector electrode records only the electrochemical process. Figure 6 shows that the recorded electrochemical reduction current in homogeneous solutions of [Fe(CN)₆]⁴⁻ (Figure 6 trace A) is greater than that of heterogeneous solutions in the presence of native TiO₂ (Figure 6 trace B), it is also greater than that of that of TiO₂/PNR (Figure 7 trace B).

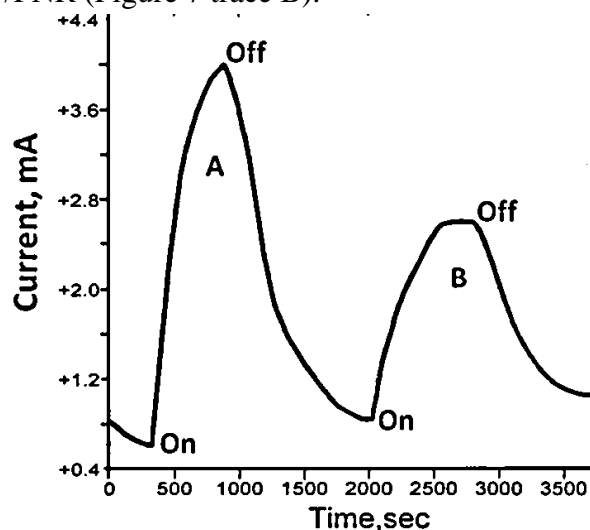


Figure 6: Photolysis of aqueous suspensions of native TiO₂ nanoparticles in 0.2 M Phosphate buffers containing 10 mM of [Fe(CN)₆]⁴⁻ (Ref.)
 A) Ref. solution 10 mM [Fe(CN)₆]⁴⁻ pH 6 0.2M phosphate buffer B) Ref + TiO₂.

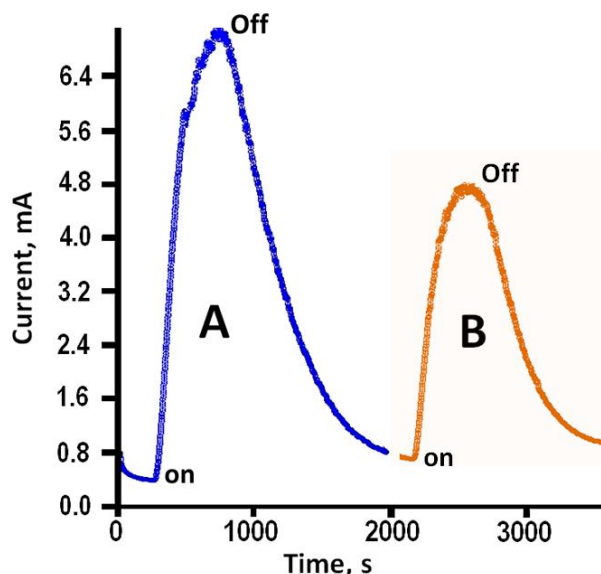
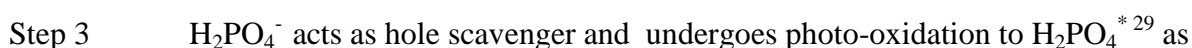
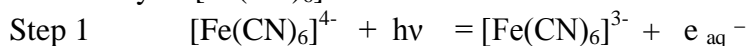


Figure 7: Photolysis of aqueous suspensions of studies IOI containing 0.2 M Phosphate buffers and 10 mM of $[\text{Fe}(\text{CN})_6]^{4-}$ A- Ref. (10 mM of $[\text{Fe}(\text{CN})_6]^{4-}$), B- Ref. + TiO_2/PNR

The smaller electrochemical reduction current in the heterogeneous system than that in homogenous system results because a portion of $[\text{Fe}(\text{CN})_6]^{3-}$ in step 1 (forthcoming) is photochemically reduced by the suspended nanoparticles. The photochemical process can be explained as follows. When SC nanoparticles were added to $[\text{Fe}(\text{CN})_6]^{4-}$ solutions, the following processes might have occurred:

The following mechanism is suggested for the photochemical reduction that causes the reversibility of $[\text{Fe}(\text{CN})_6]^{3-/4-}$ redox reaction:



Where electrons (e) are in conduction band, and hole (h) are in valence band. This step is based on the fact that the calculated e- barrier heights (1.22 eV)³⁰ for the SCs used in this study are greater than hole barrier heights (2.2 eV). This means that more negative potential will attract TiO_2 holes to PNR side. This also suggests that the hole transfer takes place first to oxidize $\text{H}_2\text{PO}_4^{1-}$ because of its higher concentration than ferrocyanide anion. Then the hole is neutralized. This suggests that the reduction of ferricyanide follows the hole consumption as shown in step 4 :

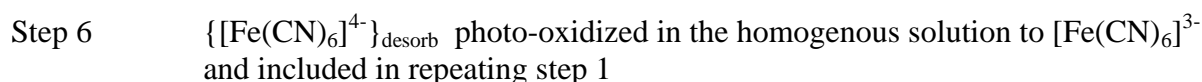


Table 2 indicates that TiO₂/PNR give better photo reduction than the native TiO₂. This can be attributed to the influence of the PNR network structure on the adsorption and desorption processes. Furthermore the lower band gap of PNR compared to that of TiO₂ increases the amount of absorbed photons. The staggered band alignment illustrated in Figure 5 B suggested that a hybrid sub-band has been developed. This sub-band facilitates the hole transfer charge transfer (aforementioned) between PNR and TiO₂ interface, because HOMO of PNR is in more positive potential than VB of TiO₂.

Table 2 - Photolysis of Aqueous 10 mM of K₄[Fe(CN)₆] (Ref) in 0.2M HPO₄²⁻ (pH =6.0)

Sample	Ref.	Ref. + TiO ₂	Ref. + TiO ₂ /PNR
EC reduction	3.270	2.221	2.000
Current , mA			
Photochem. reduction		1.049	1.300
% Photocurrent		32.07	39.75

Conclusion

At the IOI consists of TiO₂/PNR, a strong hybridization between electrons-like and hole-like sub band states in close vicinity to the Fermi energy are developed. Due to the very low hole barrier height in comparison to that of electron barrier height (1.22 eV), the charge injection/transfer mechanism took place via hole transfer. Such hole transfer initiates a reaction described in step 3 to consume the hole, while the electrons are used to complete the reduction of {[Fe(CN)₆]³⁻}_{ads}. The assembly TiO₂/PNR interface shows better photon capturing than the TiO₂ alone (table 2). PNR captures more photons of incident radiation that match its low band gap, and wastes less energy (0.15 eV) due to the relaxation of excited electrons during the fluorescence process (Figure 3 A). The long excited state life time (ca. 1.12 ns) allows for phosphate oxidation first, because of the hole supply from TiO₂'s VB, followed by reduction of Fe[(CN)]³⁻. The polymerized Neutral Red is more adhesive on TiO₂ surfaces than the monomer which merely adheres by adsorption only.

Acknowledgements

The authors would to acknowledge the support of Summer Research Institute at Indiana University Kokomo.

References

- 1- K. Gurunathan , P. Maruthamuthu and V.C. Sastri. Int J Hydrogen Energy **1997**, 22(1):57–62.
- 2- K.B. Dhanalakshmi , S. Latha , S. Anandan and P. Maruthamuthu . Int. J. Hydrogen Energy **2001**, 26:669–74.

- 3- A.K. Jana. J. Photochem Photobiol A: Chem. **2000**, 132:1–17.
- 4- K. Gurunathan. J Mol. Catal. A: Chem **2000**, 156:59–67.
- 5- R. Argazzi , N.Y.M. Iha, H. Zabri , F. Odobel and C.A. Bignozzi. Coord. Chem. Rev **2004**, 248:1299–316.
- 6- A.S. Polo , M.K. Itokazu and N.Y.M Iha. Coord. Chem. Rev **2004**, 248:1343–61.
- 7- Z.C. Bi and H.T. Tien. Int. J. Hydrogen Energy, **1984**, 9(8):717–22.
- 8- B.O. Regan and M.A. Gratzel, **Nature** 1991, 353:737–40.
- 9- R. Abe, K. Sayama and H. Arakawa. Chem. Phys. Lett. **2002**,362:441–4.
- 10- S.G. Yan and J.T. Hupp. J Phys Chem **1996**, 100:6867–70.
- 11- T.R. Heera, and L. Cindrella, Materials Science in Semiconductor Processing. **2011**, 14(2), 151-156.
- 12- Mahesh, Arumugam, J. Nanomaterials, **2011**, Article ID, 301873, 9
- 13- M. Hahlin, E.M. Johansson, S. Plogmaker , M. Odelius, P.Hagberg and S. H Rensmo, Phys. Chem. Chemical Physics, **2010**, 12(7), 1507-12.
- 14- S. Blumstengel, N. Koch , S. Sadofev , P. Schafer, H. R. Johnson , J. P. Rabe and F. Henneberger , Applied Physics Letters, **2008**, 92(19), 193303-06.
- 15- K.G. Thomas and P.V. Kamat , Acc. Chem. Res. **2003**, 36, 888-98.
- 16- K. Kasem , S. Menges, and S. Jones, Can J. Chem. **2009**, 87, 1-8.
- 17- Zhang, Qichun; Wu, Tao; Bu, Xianhui; Tran and Tri Feng, Chem. of Mate, **2008**,20(13), 4170-72.
- 18- M. Graetzel , Nature, 2001, 414, 338 342.
- 19- K. Kasem and C. Davis, Bull. Of Mat. Sciences, **2008**, 31(7), 925-929.
- 20- C. Wang, J. Zhao, X. Wang, B. Mai, G. Sheng , P. Peng and J. Fu J. Appl. Catal., B: Environ.**2002**, 39: 269–279.
- 21- D. L. Liao, C.A. Badour, and B.Q. Liao, **2008**. J. Photochem. Photobiol.A: Chem. 2008, 194: 11–19.
- 22- Y Wang, Y R Su, L Qiao, L X Liu, Q Su, C Q Zhu and X Q Liu , Nanotechnology, **2011**, 22, 225702
- 23- L.M. Peter , K.G. Wijayantha, D.J. Riley and J.P. Waggett . J. Phys. Chem. B, **2003**, 107, 8378-81.
- 24- K. Kasem, and M. Dahn. Current Science,**2010**, 99(8), 1087-92.
- 25- L.S. Roman, I.A. Hummelgen , F.C. Nart , F.C. Peres and E.L. de Sa, J. Chem .Phys., 1996, 105(23), 10614-20.
- 26- Y. Chunning, Y. Jianlong, T. Xinjun, Z. Guzhen and Z. Yue. Reactive &functional Polymers, 2006. 66, 1336-1341.
- 27- T.bak, J.Nowotny, M.Rekas and C.C. Sorrell, International J. of hydrogen Energy,**2002**, 27, pp 991-1022 .
- 28- Kasem K. Kasem and A. Finney, internat. J. Chem. **2013**, 5(3) , 76-86.
- 29- A. Mohammad , G.K.C. Low and R.W. Matthews , J. Phys. Chem.**1990**, 94, 6820-25.
- 30- T. Lana Villarreal , R. Gómez, M. Neumann-Spallart , N. Alonso-Vante and P. Salvador J. Phys. Chem. B,**2004**, 108 (39), 15172-181.